UC San Diego

UC San Diego Previously Published Works

Title

Evidence for Pro-angiogenic Functions of VEGF-Ax

Permalink

https://escholarship.org/uc/item/9zt5r1hv

Journal

Cell, 167(1)

ISSN

0092-8674

Authors

Xin, Hong

Zhong, Cuiling

Nudleman, Eric

et al.

Publication Date

2016-09-01

DOI

10.1016/j.cell.2016.08.054

Peer reviewed

eScholarship.org Powered by the California Digital Library
University of California

Matters Arising

Cell

Evidence for Pro-angiogenic Functions of VEGF-Ax

Graphical Abstract

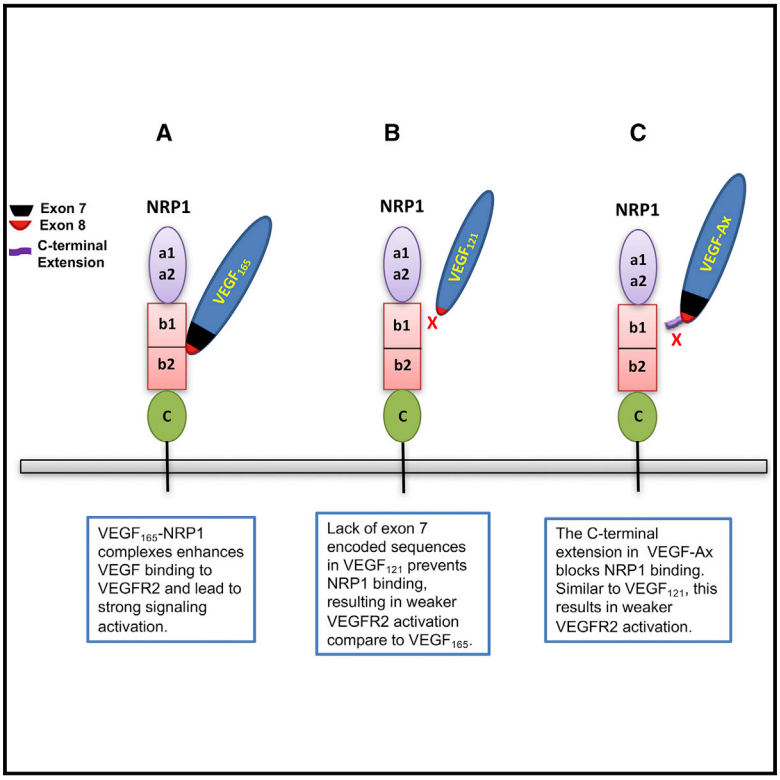

Highlights

- VEGF-Ax does not inhibit endothelial cell growth and angiogenesis
- VEGF-Ax has mitogenic, angiogenic, and permeability-enhancing functions
- The mitogenic effect of VEGF-Ax is less potent than $VEGF_{165}$
- The lower potency of VEGF-Ax is consistent with its inability to bind Neuropilin-1

Authors

Hong Xin, Cuiling Zhong, Eric Nudleman, Napoleone Ferrara

Correspondence

nferrara@ucsd.edu

In Brief

Contrary to a previous report, VEGF-Ax does not possess anti-angiogenic properties.

Xin et al., 2016, Cell *167*, 275–284
September 22, 2016 © 2016 Elsevier Inc.
http://dx.doi.org/10.1016/j.cell.2016.08.054

CellPress

Cell

Evidence for Pro-angiogenic Functions of VEGF-Ax

Hong Xin,[1] Cuiling Zhong,[1] Eric Nudleman,[1] and Napoleone Ferrara[1,2,*]
[1]University of California, San Diego, 3855 Health Sciences Drive #0819, La Jolla, CA 92093, USA
[2]Lead Contact
*Correspondence: nferrara@ucsd.edu
http://dx.doi.org/10.1016/j.cell.2016.08.054

SUMMARY

The VEGF-A isoforms play a crucial role in vascular development, and the VEGF signaling pathway is a clinically validated therapeutic target for several pathological conditions. Alternative mRNA splicing leads to the generation of multiple VEGF-A isoforms, including $VEGF_{165}$. A recent study reported the presence of another isoform, VEGF-Ax, arising from programmed readthrough translation. Compared to $VEGF_{165}$, VEGF-Ax has a 22-amino-acid extension in the COOH terminus and has been reported to function as a negative regulator of VEGF signaling in endothelial cells, with potent anti-angiogenic effects. Here, we show that, contrary to the earlier report, VEGF-Ax stimulates endothelial cell mitogenesis, angiogenesis, as well as vascular permeability. Accordingly, VEGF-Ax induces phosphorylation of key tyrosine residues in VEGFR-2. Notably, VEGF-Ax was less potent than $VEGF_{165}$, consistent with its impaired binding to the VEGF co-receptor neuropilin-1.

INTRODUCTION

Angiogenesis, the formation of new blood vessels from pre-existing vessels, is not only an essential physiological process, but also a key feature of a number of pathological processes (Folkman and Klagsbrun, 1987). Several families of mediators of angiogenesis have been described (Carmeliet and Jain, 2011; Kerbel, 2008), but it is now well established that VEGF-A is an essential regulator of this process (Ferrara and Kerbel, 2005). The binding of VEGF-A to its major tyrosine kinase receptor, VEGFR2, stimulates the proliferation of endothelial cells via the RAS/RAF/MEK/ERK signaling pathway (Herbert and Stainier, 2011; Olsson et al., 2006). The critical role of the VEGF pathway is supported by genetic studies showing that the embryos of *vegfa*$^{+/-}$ mice (Carmeliet et al., 1996; Ferrara et al., 1996) and *vegfr2* (*flk1*)$^{-/-}$ (Shalaby et al., 1995) mice have major defects in the development of the vasculature, resulting in embryonic lethality. In addition, the VEGF signaling pathway represents a validated therapeutic target for cancer and intraocular neovascular disorders (Ferrara and Adamis, 2016; Ferrara and Kerbel, 2005).

Multiple isoforms of VEGF-A exist. Alternative splicing of exons 6 and 7 of the *VEGF* gene gives rise to $VEGF_{121}$, $VEGF_{165}$, $VEGF_{189}$, and $VEGF_{206}$, the originally described isoforms (reviewed in Ferrara et al., 2003). Subsequently, less common isoforms have been reported, including $VEGF_{145}$ and $VEGF_{183}$ (Ferrara, 2004; Neufeld et al., 1999). A major difference among these isoforms is the affinity for heparin. $VEGF_{189}$ and $VEGF_{206}$ each have two heparin-binding domains encoded by exon 6 and 7, while $VEGF_{165}$ has only the exon-7-encoded heparin-binding domain (Ferrara et al., 2003). $VEGF_{121}$ is devoid of significant heparin affinity (Ferrara et al., 2003). $VEGF_{165}$ is the most frequently expressed isoform in normal tissues and in tumors (Ferrara, 2004; Neufeld et al., 1999) and has an intermediary behavior between that of the highly diffusible $VEGF_{121}$ and the strongly extracellular matrix (ECM)-bound $VEGF_{189}$. Interaction of the heparin-binding VEGF isoforms with the co-receptor Neuropilin (NRP)-1 increases their binding affinity for VEGFR-2 and potentiates the effectiveness of signal transduction (Soker et al., 1998). Also, the COOH terminus of $VEGF_{165}$ has cleavage sites for plasmin and matrix metalloproteinases (MMPs) (Ferrara, 2010). These ubiquitous proteases can generate diffusible and bioactive VEGF-A fragments (Houck et al., 1992; Keyt et al., 1996; Lee et al., 2005). Indeed, much evidence supports important roles for such proteolytic products of VEGF during angiogenesis (Ferrara, 2010).

Over the last several years, inhibitory VEGF-A isoforms have also been reported. The first was $VEGF_{165b}$ (Bates et al., 2002), a variant with an alternative 6-amino-acid end, resulting from splicing from the end of exon 7 into the 3′ untranslated region, thus replacing the sequences encoded by exon 8 (Bates et al., 2002). This molecule was reported to inhibit $VEGF_{165}$ activity in multiple contexts (Bates et al., 2002; Woolard et al., 2004), although subsequent studies have cast some doubt on such inhibitory functions and even on the existence of $VEGF_{165b}$ (Harris et al., 2012). Recently, VEGF-Ax has been described as a novel inhibitory isoform that arises from an entirely different mechanism, programmed readthrough translation (Eswarappa et al., 2014). Compared to $VEGF_{165}$, VEGF-Ax has a 22-amino-acid extension in the carboxyl (COOH) terminus. VEGF-Ax has been reported to have potent anti-angiogenic effects and to function as a negative regulator of VEGF signaling in endothelial cells. However, no clear mechanism for these inhibitory functions was elucidated (Eswarappa et al., 2014). Given the potential importance of these findings, we cloned and expressed recombinant VEGF-Ax, with the aim of deciphering the inhibitory signals emanating from the C-terminal domain unique to VEGF-Ax.

RESULTS

To investigate the effects of VEGF-Ax on endothelial cells, a DNA-fragment-encoding bovine (b) $VEGF\text{-}A_{164}$ with a COOH-terminal

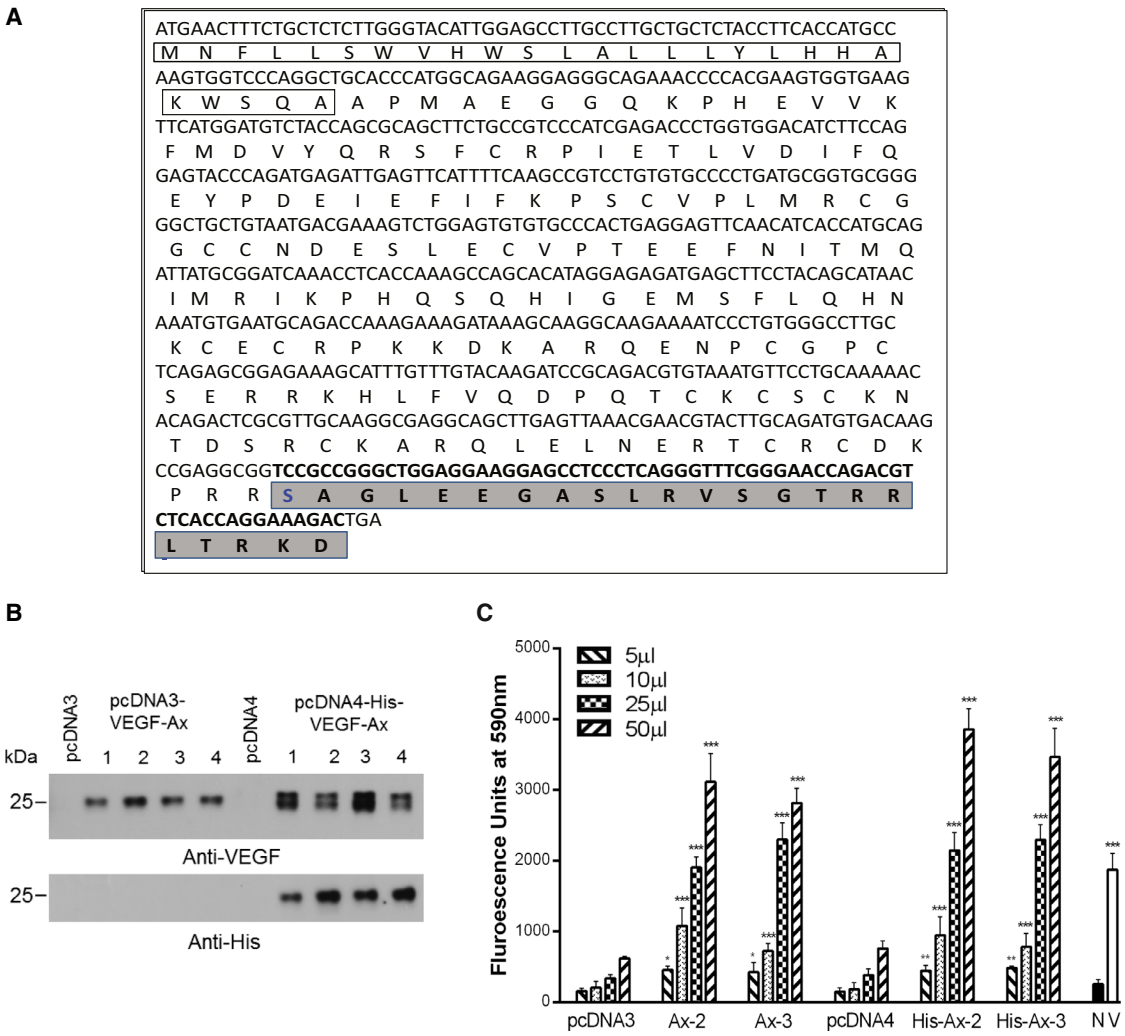

Figure 1. VEGF-Ax Cloning and Recombinant Expression

(A) Sequence of VEGF-Ax. The 22-COOH-terminal extension is highlighted in the gray box, and the blue S indicates the canonical stop codon tga replaced by tcc (serine). The signal peptide is boxed.

(B) Transient expression of VEGF-Ax. 293T cells were transfected with four individual plasmids (1–4) of untagged or his-tagged VEGF-Ax and control empty vectors (pcDNA3 and pcDNA4). After 48 hr, the cell culture media were collected and subjected to immunoblot analysis by anti-VEGF or anti-His antibodies.

(C) Effects of conditioned media of transfected cells on BCECs. BCECs were cultured in the presence of different volumes of 293T cell conditioned media, as indicated in the figure. pcDNA3 and pcDNA4 denote media conditioned by cells transfected with the empty vectors; Ax-2 and Ax-3 denote media conditioned by cells transfected with untagged VEGF-Ax; His-Ax-2 and His-Ax-3 indicate media conditioned by cells expressing His-VEGF-Ax. N and V indicate, respectively, untreated and $VEGF_{165}$ (10 ng/mL) treated groups. After 6 days, cell proliferation was analyzed. Error bars represent means ± SD. The Ax-2 and Ax-3 groups were compared to the pcDNA3 group. The His-Ax-2 and His-Ax-3 groups were compared to the pcDNA4 group. V was compared to N. The experiments were carried out in triplicate and repeated more than three times. Asterisks denote significant differences compared to the appropriate control groups (***$p < 0.001$, **$p < 0.01$, *$p < 0.05$).

extension (Eswarappa et al., 2014) was synthetized and inserted into the vectors, generating VEGF-Ax expression plasmids as described in STAR Methods. Figure 1A illustrates the sequences of the insert. The 22-amino-acid C-terminal extension is boxed and highlighted, and a blue S indicated the canonical stop codon tga replaced by tcc (serine). The presence of untagged or His-tagged (COOH terminus) VEGF-Ax in the conditioned media of transfected 293T cells was confirmed by western blot (Figure 1B).

We then tested the effects of the conditioned media on endothelial cell proliferation. As shown in Figure 1C, conditioned media from cells transiently expressing untagged or His-tagged VEGF-Ax unexpectedly resulted in robust, dilution-dependent stimulation of bovine choroidal endothelial cell (BCEC) proliferation ($p < 0.001$). Conditioned media from empty vector transfected cells had comparably little mitogenic activity. No evidence of inhibition was observed in multiple assays of independent

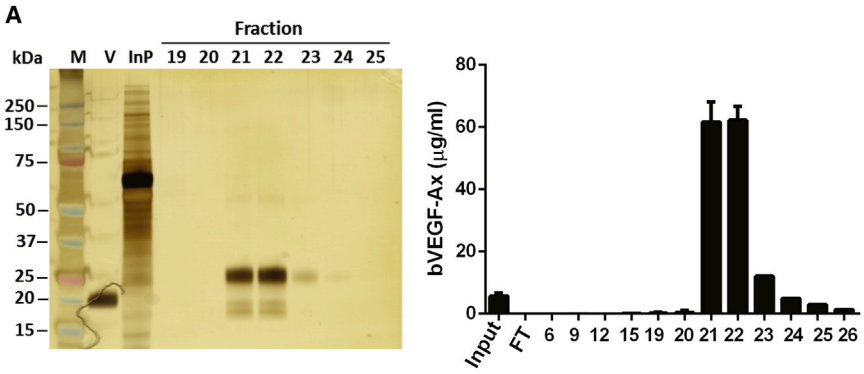

B

25 kDa band (Trypsin)

MNFLLSWVHWSLALLLYLHHAKWSQAAPMAEGGQKPHEVVKFMDVYQRSFCRPIETLVDIFQEY
PDEIEFIFKPSCVPLMRCGGCCNDESLECVPTEEFNITMQIMRIKPHQSQHIGEMSFLQHNKCE
CRPKKDKARQENPCGPCSERRKHLFVQDPQTCKCSCKNTDSRCKARQLELNERTCRCDKPRRSA
GLEEGASLRVSGTRRLTRKD

25 kDa band (GluC)

MNFLLSWVHWSLALLLYLHHAKWSQAAPMAEGGQKPHEVVKFMDVYQRSFCRPIETLVDIFQEY
PDEIEFIFKPSCVPLMRCGGCCNDESLECVPTEEFNITMQIMRIKPHQSQHIGEMSFLQHNKCE
CRPKKDKARQENPCGPCSERRKHLFVQDPQTCKCSCKNTDSRCKARQLELNERTCRCDKPRRSA
GLEEGASLRVSGTRRLTRKD

18-20 kDa band (Trypsin)

MNFLLSWVHWSLALLLYLHHAKWSQAAPMAEGGQKPHEVVKFMDVYQRSFCRPIETLVDIFQEY
PDEIEFIFKPSCVPLMRCGGCCNDESLECVPTEEFNITMQIMRIKPHQSQHIGEMSFLQHNKCE
CRPKKDKARQENPCGPCSERRKHLFVQDPQTCKCSCKNTDSRCKARQLELNERTCRCDKPRRSA
GLEEGASLRVSGTRRLTRKD

18-20 kDa band (GluC)

MNFLLSWVHWSLALLLYLHHAKWSQAAPMAEGGQKPHEVVKFMDVYQRSFCRPIETLVDIFQEY
PDEIEFIFKPSCVPLMRCGGCCNDESLECVPTEEFNITMQIMRIKPHQSQHIGEMSFLQHNKCE
CRPKKDKARQENPCGPCSERRKHLFVQDPQTCKCSCKNTDSRCKARQLELNERTCRCDKPRRSA
GLEEGASLRVSGTRRLTRKD

Figure 2. VEGF-Ax Purification and Characterization by Mass Spectrometry

(A) Purity of recombinant proteins. 5 μL aliquots of fractions from anti-VEGF mAb B20.4.1 affinity column were loaded and analyzed by silver-stained SDS-PAGE. V, InP, and #19–25 represent, respectively, $VEGF_{165}$ (250 ng), input (5μL), and the eluted fractions. Quantification of VEGF-Ax was done by measuring total bVEGF-A concentrations in the eluted fractions by ELISA.

(B) Peptide sequences identified by MS. Template sequence of bVEGF-A_{164} with a 22-amino-acid C-terminal extension mapping with MS-detected peptide sequences. The "green" indicates the sequences that are detected with over 95% confidence, the "yellow" indicates the sequence that are detected with over 50% and less than 95% confidence, the "red" is low confidence detected sequence, and "gray" is not detected sequence.

transfections. We performed most of our analyses with the untagged protein, being arguably more physiologically relevant than the His-tagged protein since it is expected to be identical to the native protein.

To purify untagged VEGF-Ax from 293T-cells-conditioned media, we performed affinity chromatography using a column coupled with anti-VEGF monoclonal antibody (mAb) B.20.4.1 (Liang et al., 2006). This mAb binds VEGF-A across species, and its binding epitope in VEGF-A closely corresponds to the receptor-binding epitope (Fuh et al., 2006). Therefore, mAb B.20.4.1 should provide an unbiased capture of functional molecular forms of VEGF-Ax in the medium. As shown in Figure 2A, this method achieved purification to near homogeneity, as assessed by silver-stained gel. We detected, in the peak fractions, a major band of approximately 25 kDa in reducing conditions, consistent with the full-length VEGF-Ax monomer. This band accounted for ~90% of the proteins by densitometry. A doublet of ~18–20 kDa was also detectable. As shown in Figure 2A, total VEGF concentrations as determined by ELISA were strongly correlated with the intensity of the bands in the gel. We made five independent preparations of untagged VEGF-Ax, with very similar results.

For purification of His-VEGF-Ax, His-Trap^R (Ni-Sepharose) columns were used and three independent purifications were performed. The recovery of purified His-VEGF-Ax, as assessed by ELISA, was comparable with that of the anti-VEGF antibody affinity column (data not shown). It is noteworthy that only His-VEGF-Ax with an intact C terminus can bind the His-Trap column, while cleaved forms devoid of His-tag would not be retained.

We performed mass spectrometry (MS) analysis to structurally characterize the purified untagged VEGF-Ax proteins. The above mentioned higher and lower molecular mass bands were cut and submitted for analysis. As shown in Figure 2B, several peptide sequences (up to 67 amino acids) were identified in both samples with over 95% confidence, and all of those peptide sequences matched the sequence of bVEGF-A_{164} (Leung et al., 1989). A partial amino-acid sequence of the C-terminal extension "SAGLEEGASL" was detected with over 95% confidence in the 25 kDa sample digested by trypsin. GluC digestion yielded another partial sequence of the C-terminal extension "GASLRVSGTRRLTRKD" with over 95% confidence, showing overlap in "GASL." Therefore, the entire sequence of the 22-amino-acid extension unique to VEGF-Ax was unambiguously detected in the major protein band using this two-enzyme digestion strategy. The lower band sample was consistent with C-terminal proteolytic products of VEGF-Ax lacking the 22-amino-acid extension.

We tested purified VEGF-Ax in endothelial cell mitogenic assays. BCECs and BRECs (bovine retinal endothelial cells) were cultured in the presence of different concentrations of VEGF-Ax, with or without $VEGF_{165}$. Untagged VEGF-Ax significantly ($p < 0.001$) induced proliferation of both BCECs (Figure 3A) and BRECs (Figure 3B) in a dose-dependent manner. The magnitude of the stimulation was 50%–70% of that obtained with $VEGF_{165}$. Similarly, His-tagged VEGF-Ax significantly ($p < 0.001$) induced BCEC proliferation (Figure 3C). As shown in Figure S1 (related to Figure 3), untagged and His-tagged VEGF-Ax had a very similar ability to stimulate phosphorylation in VEGFR2 Y1175 and ERK1/2 activation. Importantly, no inhibition of $VEGF_{165}$-stimulated endothelial cell proliferation was observed in the presence of untagged or His-tagged VEGF-Ax. To test

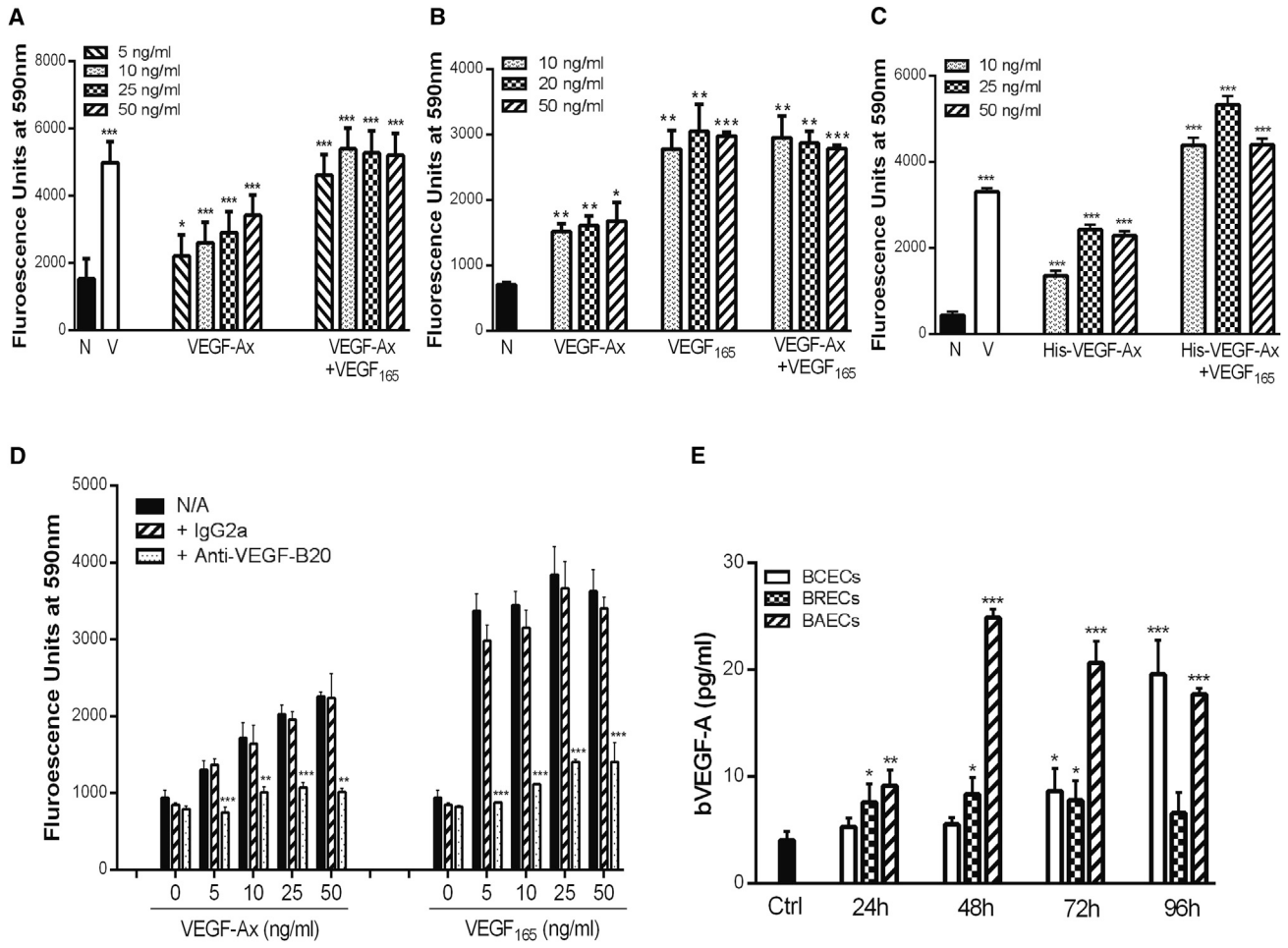

Figure 3. Mitogenic Effects of Untagged and His-tagged Recombinant VEGF-Ax and Release of Endogenous VEGF from Bovine Endothelial Cells

(A–C) Effects of VEGF-Ax on bovine endothelial cell proliferation. BCECs (A and C) and BRECs (B) were cultured in the presence of different concentrations of untagged (A and B) or His-tagged (C) VEGF-Ax, with or without 10 ng/mL $VEGF_{165}$. After 5–6 days, cell proliferation was determined by fluorescence readings at 590 nm. N and V indicate, respectively, untreated and $VEGF_{165}$ (10 ng/mL) treated groups. Asterisks denote significant differences compared to control untreated groups.

(D) Specificity of the effects of VEGF-Ax on BCECs. 2 μg/mL of anti-VEGF mAb B20.4.1 or isotype control IgG2a was added 1 hr before treatment with VEGF-Ax or $VEGF_{165}$ at the indicated concentrations. Asterisks denote mAb B20.4.1 groups that are significantly different from the control IgG2a groups (***$p < 0.001$, **$p < 0.01$).

(E) Release of endogenous VEGF-A by bovine endothelial cells. BCECs, BRECs, and BAECs were cultured in low glucose DMEM supplemented with 2.5% bovine calf serum, and the media were collected at 24, 48, 72, and 96 hr, respectively, and concentrated 26-fold by 10k Millipore Amicon centrifugal columns prior to ELISA. All of the experiments were carried out in triplicate and repeated at least three times. Asterisks denote groups that are significantly different from the control medium (no cells) groups (***$p < 0.001$, **$p < 0.01$, *$p < 0.05$).

the specificity of the effects of VEGF-Ax, we used mAb B20.4.1. Addition of mAb B20.4.1 almost completely ($p < 0.001$) inhibited VEGF-Ax- or $VEGF_{165}$-induced BCEC proliferation. In contrast, a control immunoglobulin G (IgG) had no effect on BCEC proliferation stimulated by VEGF-Ax or $VEGF_{165}$ (Figure 3D). To determine VEGF-A release from bovine endothelial cells, we measured total VEGF-A by ELISA in the cell culture media collected at various time points (Figure 3E). We found that the amounts of VEGF-A were very low; the highest concentration was 25 pg/mL in BAECs (bovine aortic endothelial cells) and BCECs, and it was almost undetectable in BRECs.

Migration of human umbilical vein endothelial cells (HUVECs) was also assessed. As shown in Figure 4A, the number of migrated cells significantly ($p < 0.01$) increased in the presence of VEGF-Ax or $VEGF_{165}$. In this assay, the magnitude of the effect of the two ligands was comparable. No inhibition of $VEGF_{165}$-induced endothelial cell migration was observed when VEGF-Ax and $VEGF_{165}$ were combined.

To further confirm the effects of VEGF-Ax on endothelial cell proliferation and migration, BCEC monolayers were mechanically wounded. As shown in Figure 4B, in the presence of $VEGF_{165}$, VEGF-Ax, or both, cell proliferation and migration

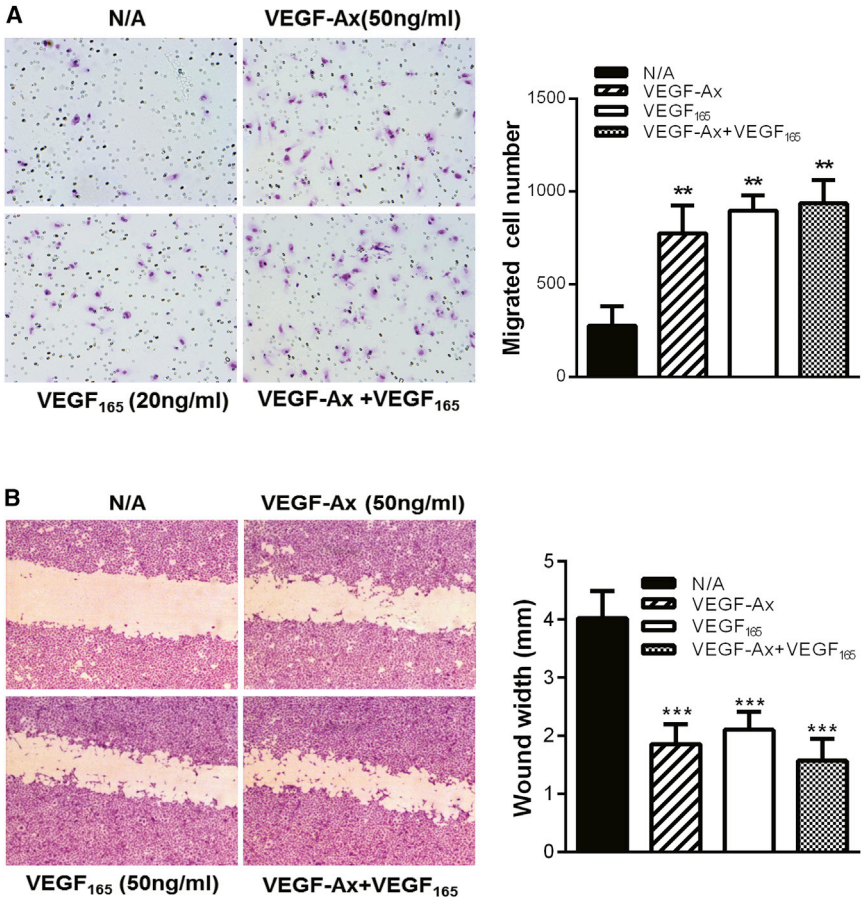

Figure 4. Effects of VEGF-Ax on Chemotaxis by Trans-Well and Scratch Assays

(A) HUVECs migration by trans-well analysis. Serum-starved HUVECs were incubated in the presence of 50 ng/mL of VEGF-Ax, 20 ng/mL of $VEGF_{165}$, or a combination of both ligands at the above concentrations. Representative pictures were taken under the light microscope at 100× magnification showing the migrated cells. Quantification of the migrated cells was done by counting whole area of the insert at 40× magnifications. The experiments were carried out in triplicate, and the error bars represent means ± SD from three independent experiments.

(B) Migration and proliferation analyzed by scratch assay. Subconfluent BCEC monolayers in 6-well plates were serum starved and wounded, followed by addition of 50 ng/mL VEGF-Ax, 50 ng/mL $VEGF_{165}$, or a combination of both ligands, each at 50 ng/mL in duplicate wells. 48 hr later, images were acquired by ZEISS Discovery V8 SteREO microscope equipped with PixeLINK Megapixel FireWire camera. Quantification of wound closure was done using AxioVision LE Rel.4.4 software. Six measurements were taken of each image, and values are means ± SD from four independent studies. Asterisks denote significant differences compared to no addition (N/A) groups (***$p < 0.001$, **$p < 0.01$).

toward the gap between the wound edges were evident, resulting in a significantly narrower gap compared to the control group. There was no evidence that VEGF-Ax antagonized the activity of $VEGF_{165}$.

Explanted mouse choroidal tissue provides a model for studying microvascular proliferation (Shao et al., 2013). We used this assay to evaluate the pro-angiogenic effect of $VEGF_{165}$, VEGF-Ax, and these molecules in combination. In pilot experiments, we tested various concentrations of $VEGF_{165}$ and identified 25 ng as a concentration that strongly stimulates vessel sprouting relative to buffer control. When compared to 25 ng of VEGF-Ax, an equivalent amount of vessel proliferation over the same time period was observed. No difference in the density or extent of vessel proliferation was identified (Figure 5A). Furthermore, increasing the concentrations of VEGF-Ax or combining with lower concentration of $VEGF_{165}$ did not induce further stimulation (or inhibition) of vessel proliferation. These data suggest very similar effects of $VEGF_{165}$ and VEGF-Ax on choroidal explant vascular proliferation.

One of the known activities of VEGF is the rapid induction of vascular permeability from an intact endothelium (Senger et al., 1983). Therefore, we tested the ability of VEGF-Ax to induce vascular permeability in the Miles assay. As shown in Figure 5B, VEGF-Ax induced dye extravasation in a dose-dependent manner compared to PBS control (dose 0). $VEGF_{165}$, as expected, strongly induced dye leakage. Administration of 50 ng of $VEGF_{165}$ combined with different doses of VEGF-Ax (25–250ng) induced more dye extravasation compared to $VEGF_{165}$ or VEGF-Ax treatment alone.

After this work was essentially completed, human VEGF-Ax became available from R&D Systems. As shown in Figure 6, R&D Systems VEGF-Ax and our purified VEGF-Ax had comparable mitogenic effects on bovine endothelial cells and did not inhibit $VEGF_{165}$-stimulated proliferation, even at a molar ratio of ~10:1. We also tested, in the same assay, $VEGF_{165b}$, which also stimulated endothelial cell proliferation and did not inhibit $VEGF_{165}$-stimulated growth (Figure 6).

Given the finding that VEGF-Ax has both mitogenic and permeabilizing effects, we examined the phosphorylation status of two key tyrosine residues in VEGFR2, Y1175 and Y951, which have been implicated, respectively, in the induction of endothelial cell proliferation (Sakurai et al., 2005) and of vascular permeability (Li et al., 2016). As shown in Figure 7A, VEGF-Ax purified in our laboratory or VEGF-Ax purchased from R&D Systems induced phosphorylation of both Y1175 and Y951 in VEGFR2. $VEGF_{165b}$ also induced phosphorylation of both tyrosine residues (Figure 7A). Since p44/42 MAPK (ERK1/2) is downstream of VEGFR2 activation, we also tested the phosphorylation status of ERK1/2. In agreement with the VEGFR2 tyrosine phosphorylation data, VEGF-Ax, $VEGF_{165}$, and, to a lesser extent, $VEGF_{165b}$ stimulated p-ERK1/2 (Figure 7A).

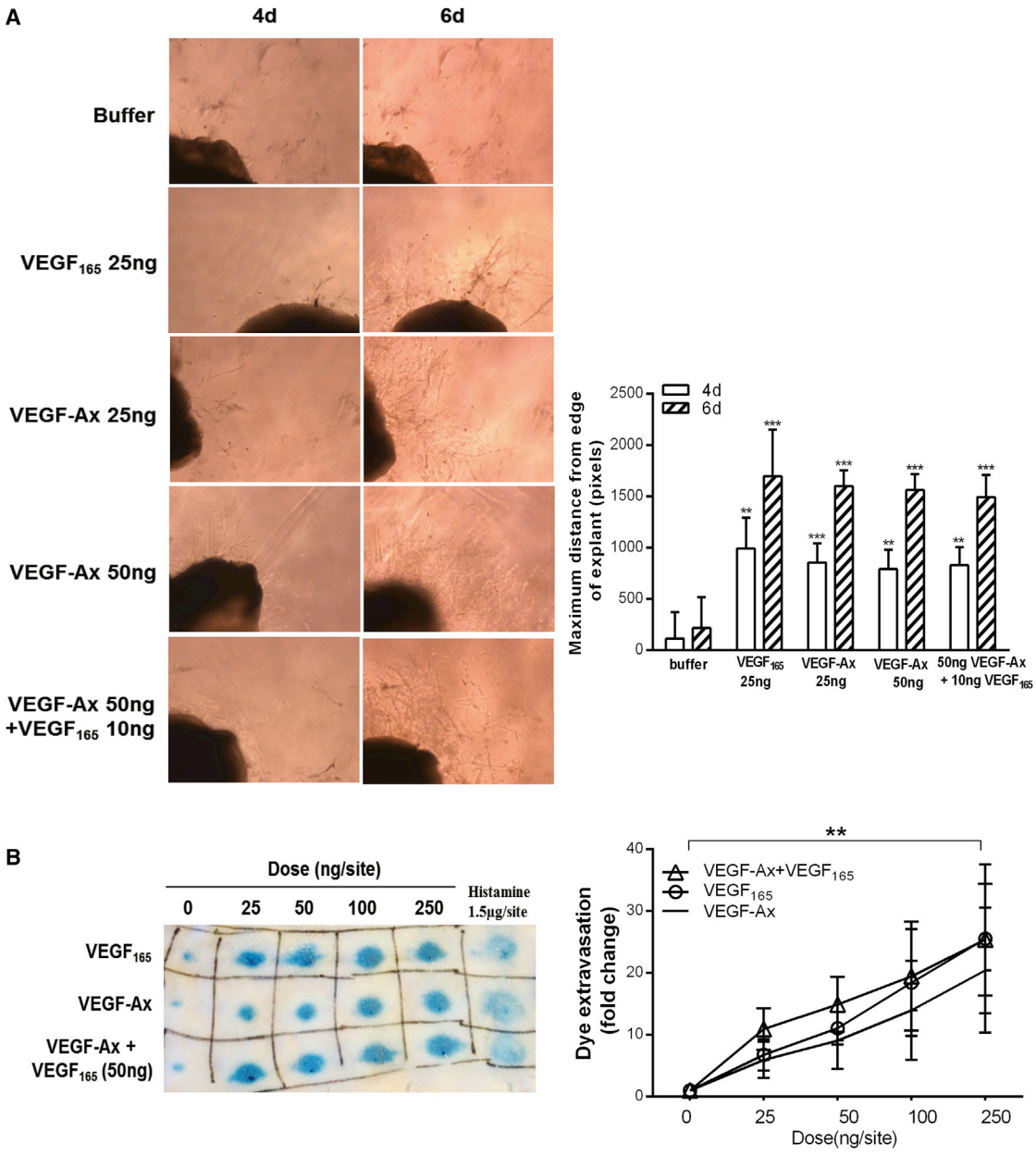

Figure 5. Angiogenic and Permeability Enhancing Effects by VEGF-Ax

(A) Induction of mouse choroidal explants by VEGF-Ax. Vascular proliferation from primary choroidal explants at 4 and 6 days post-seeding are shown in the representative pictures. Supplements were added to each sample as indicated. Quantification of the growth of vascular sprouts was performed using Axiovision software. The values are means ± SD from five independent eyes. Asterisks denote treatment groups that are significantly different from the buffer control groups (***$p < 0.001$, **$p < 0.01$).

(B) Induction of vascular permeability by VEGF-Ax in the Miles assay. Representative picture of guinea pig skin showing dye extravasation in response to the indicated treatments. 1.5 μg/site of histamine served as a positive control. Quantification of dye extravasation was carried out using ImageJ software. Values shown are means ± SD from five independent guinea pigs. Asterisks denote significant differences between indicated treatment (25–250 ng/site) and untreated group (dose 0). All treatment groups were significantly different from the untreated group. (***$p < 0.001$, **$p < 0.01$, *$p < 0.05$).

Using an ELISA-based approach, we sought to determine whether VEGF-Ax is able to compete with biotinylated $VEGF_{165}$ for NRP1 binding. Unlike $VEGF_{165}$, neither $VEGF_{121}$ nor VEGF-Ax significantly competed with biotinylated $VEGF_{165}$ (Figure 7B).

DISCUSSION

By alternative mRNA splicing, multiple VEGF-A isoforms are generated, including $VEGF_{121}$, $VEGF_{165}$, and $VEGF_{189}$. (Houck et al., 1991; Tischer et al., 1991) These isoforms have been

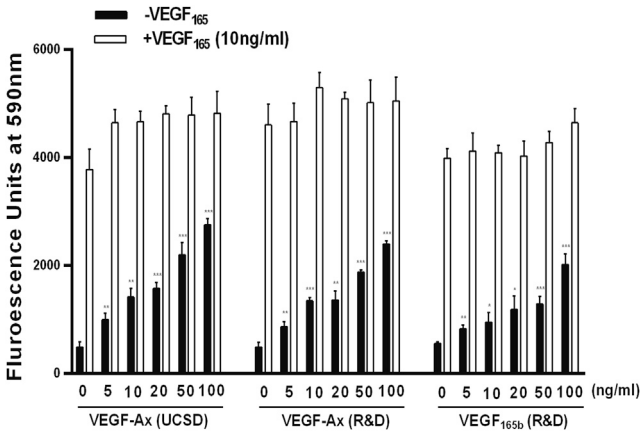

Figure 6. Effects of VEGF Variants on Bovine Choroidal Endothelial Cell Proliferation

Different concentrations of VEGF-Ax purified in our laboratory (UCSD) or VEGF-Ax from R&D Systems were tested in the presence or absence of 10 ng/mL $VEGF_{165}$. $VEGF_{165b}$ was also tested under similar conditions. The experiments were carried out in triplicate and repeated three times. Data shown are means ± SD. Asterisks denote significant differences compared to no treatment (0) groups (***$p < 0.001$, **$p < 0.01$, *$p < 0.05$).

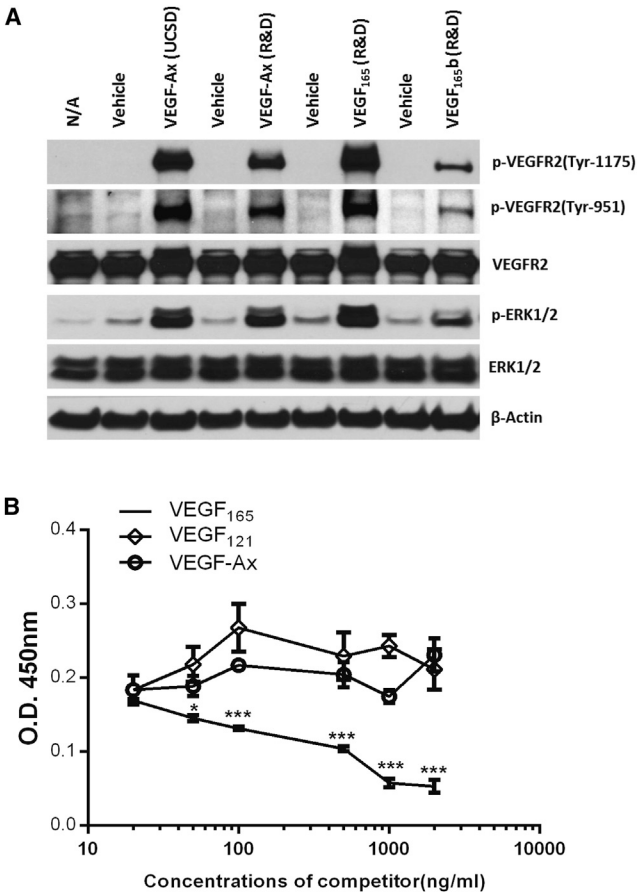

Figure 7. VEGF-Ax Induces VEGFR2 Signaling and Fails to Bind NRP1

(A) Western blot showing increased phosphorylation of VEGFR2 Y1175 and Y951 and ERK1/2 activation induced by VEGF-A variants. Serum-starved HUVECs were stimulated for 10 minutes with 50 ng/mL of VEGF-Ax purified in our laboratory (UCSD), commercial VEGF-Ax (R&D), $VEGF_{165b}$, or wild-type $VEGF_{165}$. Each VEGF variant was compared to its appropriate vehicle control. N/A, no addition. Equal amounts of whole-cell lysates were subjected to SDS-PAGE and then blotted with the indicated antibodies.

(B) Solid-phase NRP1 binding assay. $VEGF_{165}$, but not VEGF-Ax or $VEGF_{121}$, is able to compete with biotinylated $VEGF_{165}$ for binding to NRP1-Fc. The assays were carried out in duplicate wells. The values shown are means ± SD from three independent studies. Asterisks denote significant differences compared with control buffer (***$p < 0.001$, *$p < 0.05$).

characterized as having pro-angiogenic functions in vitro and in vivo, although the degrees of potency varied depending on the C-terminal sequences and the ability to bind NRP1 (Carmeliet et al., 1999; Houck et al., 1992; Keyt et al., 1996; Soker et al., 1998).

In 2002, Bates et al. (2002) reported the existence of an additional isoform, $VEGF_{165b}$, which was reported to have paradoxically anti-angiogenic effects and the ability to antagonize VEGF-A-induced effects (Bates et al., 2002). Potentially, this study provided a new paradigm of VEGF-A regulation and function. However, these findings have not been without controversy, as some groups were unable to confirm antagonistic properties of $VEGF_{165b}$ and, instead, reported weak agonistic activities (Catena et al., 2010; Kawamura et al., 2008). In the present study, we also found that $VEGF_{165b}$ has mitogenic effects on endothelial cells.

Recently, Eswarappa et al. (2014) have described a novel anti-angiogenic VEGF-A isoform, VEGF-Ax, resulting from programmed readthrough translation. VEGF-Ax includes a 22-amino-acid C-terminal extension due to reading of the canonical stop codon as a serine. Readthrough translation, which occurs primarily in viruses and fungi but has been observed also in mammals, consists of decoding a canonical stop codon as a sense codon due to the pairing of a near-cognate aminoacyl-tRNA to the stop codon in the ribosomal A site instead of eRF1(Beier and Grimm, 2001; Firth and Brierley, 2012; Namy et al., 2004). This process results in the generation of C-extended proteins, thus potentially enhancing functional diversity and even affecting cellular localization (Schueren et al., 2014). It is generally agreed that such C-terminally extended proteins represent low-abundance products that account for a small fraction of the translated proteins in mammals (Schueren et al., 2014).

Intriguingly, VEGF-Ax was characterized as an antagonist and proposed to function as an endogenous inhibitor of VEGF-mediated angiogenesis (Eswarappa et al., 2014). However, an initial analysis of the 22-amino-acid extension unique to VEGF-Ax does not reveal any known domain or motif that might account for such inhibitory effects. Four out of 22 residues are hydrophobic, and 7 out of 22 are charged. Therefore, this extension might potentially bind to heparin.

The authors suggested that the reported inhibitory effects are related to the inability of VEGF-Ax to bind NRP1 (Eswarappa et al., 2014). Indeed, we have been able to confirm that VEGF-Ax has a markedly reduced if not undetectable ability to compete with $VEGF_{165}$ for NRP1 binding. This finding is somewhat surprising, considering that, unlike $VEGF_{165b}$ (Kawamura et al.,

2008), VEGF-Ax has all the structural elements required to bind NRP1 (Vander Kooi et al., 2007). It is generally accepted that the C-terminal exon-8-encoded sequences in VEGF represent the site of direct interaction between $VEGF_{165}$ and NRP1, although sequences encoded by exon 7 are required to extend this region to effectively gain access to the NRP1 dimer (Vander Kooi et al., 2007). Thus, it appears that the 22-amino-acid extension in VEGF-Ax blocks or disrupts this interaction. Structural studies will be required to define these blocking effects. However, the hypothesis that loss of NRP1 binding confers antagonistic or inhibitory properties lacks structural basis. Indeed, $VEGF_{121}$ (which lacks exon-7-encoded sequences), C-terminal proteolytic fragments of $VEGF_{165}$ resulting from plasmin (Houck et al., 1992; Keyt et al., 1996), or matrix metalloproteinase (MMP)3 (Lee et al., 2005) cleavage and VEGF mutants (Li et al., 2000) lacking all exon-7- and exon-8-encoded sequences have reduced or absent ability to bind NRP1 (Soker et al., 1998; Vander Kooi et al., 2007). Nevertheless, all of these variants have been shown to induce VEGFR2 phosphorylation, mitogenesis, angiogenesis, and vascular permeability, albeit with reduced potency compared to intact $VEGF_{165}$ (Houck et al., 1992; Keyt et al., 1996; Lee et al., 2005; Li et al., 2000; Park et al., 1993).

To gain some mechanistic insights into the reported anti-angiogenic effects of VEGF-Ax, we cloned and expressed both untagged and His-tagged VEGF-Ax and purified the recombinant proteins. We were able to document by MS of the untagged protein, purified by affinity chromatography using an anti-VEGF function-blocking antibody, that the major VEGF-Ax band has an intact 22-amino-acid extension. A much-less-abundant molecular form was consistent with proteolysis of VEGF-Ax at the C terminus, a well-known feature of the VEGF proteins in vitro and in vivo (Ferrara, 2010). Therefore, it is likely that the VEGF-Ax purified by this approach more closely reflects the heterogeneity occurring in the microenvironment, as compared to His-VEGF-Ax purified by His-Trap columns, since an intact C terminus is required to bind the column in this case. Nevertheless, purified untagged and His-tagged VEGF-Ax proteins had very similar mitogenic effects and abilities to induce VEGFR2 tyrosine phosphorylation and ERK1/2 activation.

In contrast with the findings by Eswarappa et al. (2014), we were unable to detect any inhibition of either basal or VEGF-stimulated endothelial cell growth even with a VEGF-Ax/$VEGF_{165}$ ~10:1 molar ratio. Using a variety of in vitro, ex vivo, and in vivo bioassays, we documented clear agonistic activities of VEGF-Ax. Importantly, these effects were observed across a broad spectrum of experimental conditions, ranging from 10% serum to serum-free conditions. In agreement with these findings, VEGF-Ax induced phosphorylation of two key VEGFR2 tyrosine residues, Y951 and Y1175.

The finding that the potency of VEGF-Ax was lower than that of $VEGF_{165}$ is entirely consistent with impaired NRP1 binding. Indeed, several studies have shown that NRP1 forms complexes with $VEGF_{165}$, which enhance its binding affinity for VEGFR2 (Neufeld et al., 2002; Soker et al., 1998, 2002; Whitaker et al., 2001). Accordingly, as already noted, VEGF-A isoforms or proteolytic fragments of VEGF-A devoid of NRP1 binding have reduced biological potency (Houck et al., 1992; Keyt et al., 1996; Lee et al., 2005; Li et al., 2000; Park et al., 1993).

Eswarappa et al. (2014) concluded, on the basis of western blots, that VEGF-Ax is abundantly released in the supernatants of cultured bovine endothelial cells. The authors speculated that VEGF-Ax is responsible for preventing growth and maintaining endothelial cells in a quiescent state. However, using an ELISA, we found that the total amounts of VEGF-A released by three different bovine endothelial cell types are exceedingly low or undetectable, raising the question of whether such amounts may even be biologically significant. Specific and quantitative methodologies are clearly needed to accurately estimate the concentrations of VEGF-Ax in endothelial cells and in other cell types, in vitro and in vivo.

How can we account for the conflicting findings? One could speculate that the inhibitory function of VEGF-Ax associated with the C terminus might have been impaired or disrupted in the course of the purification procedures employed by us. However, the finding that the starting material, the unprocessed conditioned media of transfected cells expressing untagged or His-tagged VEGF-Ax, consistently induced endothelial cell proliferation clearly argues against the hypothesis. Importantly, the commercially available VEGF-Ax had similar mitogenic effects to the proteins prepared in our laboratory. An alternative possibility is that the reported inhibitory effects (Eswarappa et al., 2014) may be mediated by contaminants or impurities. In this context, when screening a library of human secreted proteins (Clark et al., 2003) to identify growth stimulators and inhibitors for bovine endothelial cells (LeCouter et al., 2001), we observed a surprisingly high rate of inhibitory "hits" using an early version of the library. Most of these "hits" were not confirmed with more stringently purified proteins. It became apparent that endothelial cell growth could be easily inhibited by a variety of impurities, including protein aggregates or traces of imidazole, a buffer typically used to elute His-tagged proteins from Ni-Sepharose columns. It remains to be established whether any of these possibilities account for the conflicting results.

STAR★METHODS

Detailed methods are provided in the online version of this paper and include the following:

- KEY RESOURCES TABLE
- CONTACT FOR REAGENT AND RESOURCE SHARING
- EXPERIMENTAL MODELS AND SUBJECT DETAILS
  - Mice
  - Guinea Pigs
  - Cells
- METHOD DETAILS
  - Plasmid Construction and Transfection
  - Conditioned Media Preparation and VEGF-A ELISA
  - Western Blots
  - Bovine Endothelial Cell Proliferation Assays
  - VEGF Release from Cultured Bovine Endothelial Cells
  - HUVEC Migration Assay
  - Scratch Assay
  - Mouse Choroidal Explant Assay
  - Vascular Permeability Assay
  - Purification of VEGF-Ax

- Structural Analysis
- Solid-Phase NRP1 Binding Assay

- QUANTIFICATION AND STATISTICAL ANALYSIS

SUPPLEMENTAL INFORMATION

Supplemental Information includes one figure and can be found with this article online at http://dx.doi.org/10.1016/j.cell.2016.08.054.

AUTHOR CONTRIBUTIONS

H.X., C.Z., E.N., and N.F. designed and performed research and analyzed data. H.X. and N.F. wrote the paper. N.F. oversaw the project.

ACKNOWLEDGMENTS

We thank Majid Ghassemian and the UCSD Mass Spectrometry Facility for outstanding support. We thank Daniel Leahy (Univ. of Texas, Austin) for helpful discussions on the structural basis of the VEGF-A-NRP1 interaction.

Received: June 2, 2016
Revised: August 7, 2016
Accepted: August 19, 2016
Published: September 22, 2016

REFERENCES

Bates, D.O., Cui, T.G., Doughty, J.M., Winkler, M., Sugiono, M., Shields, J.D., Peat, D., Gillatt, D., and Harper, S.J. (2002). VEGF165b, an inhibitory splice variant of vascular endothelial growth factor, is down-regulated in renal cell carcinoma. Cancer Res. *62*, 4123–4131.

Beier, H., and Grimm, M. (2001). Misreading of termination codons in eukaryotes by natural nonsense suppressor tRNAs. Nucleic Acids Res. *29*, 4767–4782.

Carmeliet, P., and Jain, R.K. (2011). Molecular mechanisms and clinical applications of angiogenesis. Nature *473*, 298–307.

Carmeliet, P., Ferreira, V., Breier, G., Pollefeyt, S., Kieckens, L., Gertsenstein, M., Fahrig, M., Vandenhoeck, A., Harpal, K., Eberhardt, C., et al. (1996). Abnormal blood vessel development and lethality in embryos lacking a single VEGF allele. Nature *380*, 435–439.

Carmeliet, P., Ng, Y.-S., Nuyens, D., Theilmeier, G., Brusselmans, K., Cornelissen, I., Ehler, E., Kakkar, V.V., Stalmans, I., Mattot, V., et al. (1999). Impaired myocardial angiogenesis and ischemic cardiomyopathy in mice lacking the vascular endothelial growth factor isoforms VEGF164 and VEGF188. Nat. Med. *5*, 495–502.

Catena, R., Larzabal, L., Larrayoz, M., Molina, E., Hermida, J., Agorreta, J., Montes, R., Pio, R., Montuenga, L.M., and Calvo, A. (2010). $VEGF_{121}b$ and $VEGF_{165}b$ are weakly angiogenic isoforms of VEGF-A. Mol. Cancer *9*, 320.

Clark, H.F., Gurney, A.L., Abaya, E., Baker, K., Baldwin, D., Brush, J., Chen, J., Chow, B., Chui, C., Crowley, C., et al. (2003). The secreted protein discovery initiative (SPDI), a large-scale effort to identify novel human secreted and transmembrane proteins: a bioinformatics assessment. Genome Res. *13*, 2265–2270.

Eswarappa, S.M., Potdar, A.A., Koch, W.J., Fan, Y., Vasu, K., Lindner, D., Willard, B., Graham, L.M., DiCorleto, P.E., and Fox, P.L. (2014). Programmed translational readthrough generates antiangiogenic VEGF-Ax. Cell *157*, 1605–1618.

Ferrara, N. (2004). Vascular endothelial growth factor: basic science and clinical progress. Endocr. Rev. *25*, 581–611.

Ferrara, N. (2010). Binding to the extracellular matrix and proteolytic processing: two key mechanisms regulating vascular endothelial growth factor action. Mol. Biol. Cell *21*, 687–690.

Ferrara, N., and Adamis, A.P. (2016). Ten years of anti-vascular endothelial growth factor therapy. Nat. Rev. Drug Discov. *15*, 385–403.

Ferrara, N., and Kerbel, R.S. (2005). Angiogenesis as a therapeutic target. Nature *438*, 967–974.

Ferrara, N., Carver-Moore, K., Chen, H., Dowd, M., Lu, L., O'Shea, K.S., Powell-Braxton, L., Hillan, K.J., and Moore, M.W. (1996). Heterozygous embryonic lethality induced by targeted inactivation of the VEGF gene. Nature *380*, 439–442.

Ferrara, N., Gerber, H.P., and LeCouter, J. (2003). The biology of VEGF and its receptors. Nat. Med. *9*, 669–676.

Firth, A.E., and Brierley, I. (2012). Non-canonical translation in RNA viruses. J. Gen. Virol. *93*, 1385–1409.

Folkman, J., and Klagsbrun, M. (1987). Angiogenic factors. Science *235*, 442–447.

Fuh, G., Wu, P., Liang, W.C., Ultsch, M., Lee, C.V., Moffat, B., and Wiesmann, C. (2006). Structure-function studies of two synthetic anti-vascular endothelial growth factor Fabs and comparison with the Avastin Fab. J. Biol. Chem. *281*, 6625–6631.

Gille, H., Kowalski, J., Li, B., LeCouter, J., Moffat, B., Zioncheck, T.F., Pelletier, N., and Ferrara, N. (2001). Analysis of biological effects and signaling properties of Flt-1 (VEGFR-1) and KDR (VEGFR-2). A reassessment using novel receptor-specific vascular endothelial growth factor mutants. J. Biol. Chem. *276*, 3222–3230.

Harris, S., Craze, M., Newton, J., Fisher, M., Shima, D.T., Tozer, G.M., and Kanthou, C. (2012). Do anti-angiogenic VEGF (VEGFxxxb) isoforms exist? A cautionary tale. PLoS ONE *7*, e35231.

Herbert, S.P., and Stainier, D.Y. (2011). Molecular control of endothelial cell behaviour during blood vessel morphogenesis. Nat. Rev. Mol. Cell Biol. *12*, 551–564.

Houck, K.A., Ferrara, N., Winer, J., Cachianes, G., Li, B., and Leung, D.W. (1991). The vascular endothelial growth factor family: identification of a fourth molecular species and characterization of alternative splicing of RNA. Mol. Endocrinol. *5*, 1806–1814.

Houck, K.A., Leung, D.W., Rowland, A.M., Winer, J., and Ferrara, N. (1992). Dual regulation of vascular endothelial growth factor bioavailability by genetic and proteolytic mechanisms. J. Biol. Chem. *267*, 26031–26037.

Kawamura, H., Li, X., Harper, S.J., Bates, D.O., and Claesson-Welsh, L. (2008). Vascular endothelial growth factor (VEGF)-A165b is a weak in vitro agonist for VEGF receptor-2 due to lack of coreceptor binding and deficient regulation of kinase activity. Cancer Res. *68*, 4683–4692.

Kerbel, R.S. (2008). Tumor angiogenesis. N. Engl. J. Med. *358*, 2039–2049.

Keyt, B.A., Berleau, L.T., Nguyen, H.V., Chen, H., Heinsohn, H., Vandlen, R., and Ferrara, N. (1996). The carboxyl-terminal domain (111-165) of vascular endothelial growth factor is critical for its mitogenic potency. J. Biol. Chem. *271*, 7788–7795.

LeCouter, J., Kowalski, J., Foster, J., Hass, P., Zhang, Z., Dillard-Telm, L., Frantz, G., Rangell, L., DeGuzman, L., Keller, G.-A., et al. (2001). Identification of an angiogenic mitogen selective for endocrine gland endothelium. Nature *412*, 877–884.

Lee, S., Jilani, S.M., Nikolova, G.V., Carpizo, D., and Iruela-Arispe, M.L. (2005). Processing of VEGF-A by matrix metalloproteinases regulates bioavailability and vascular patterning in tumors. J. Cell Biol. *169*, 681–691.

Leung, D.W., Cachianes, G., Kuang, W.J., Goeddel, D.V., and Ferrara, N. (1989). Vascular endothelial growth factor is a secreted angiogenic mitogen. Science *246*, 1306–1309.

Li, B., Fuh, G., Meng, G., Xin, X., Gerritsen, M.E., Cunningham, B., and de Vos, A.M. (2000). Receptor-selective variants of human vascular endothelial growth factor. Generation and characterization. J. Biol. Chem. *275*, 29823–29828.

Li, X., Padhan, N., Sjöström, E.O., Roche, F.P., Testini, C., Honkura, N., Sáinz-Jaspeado, M., Gordon, E., Bentley, K., Philippides, A., et al. (2016). VEGFR2 pY949 signalling regulates adherens junction integrity and metastatic spread. Nat. Commun. *7*, 11017.

Liang, W.C., Wu, X., Peale, F.V., Lee, C.V., Meng, Y.G., Gutierrez, J., Fu, L., Malik, A.K., Gerber, H.P., Ferrara, N., et al. (2006). Cross-species vascular endothelial growth factor (VEGF)-blocking antibodies completely inhibit the

growth of human tumor xenografts and measure the contribution of stromal VEGF. J. Biol. Chem. *281*, 951–961.

Namy, O., Rousset, J.P., Napthine, S., and Brierley, I. (2004). Reprogrammed genetic decoding in cellular gene expression. Mol. Cell *13*, 157–168.

Neufeld, G., Cohen, T., Gengrinovitch, S., and Poltorak, Z. (1999). Vascular endothelial growth factor (VEGF) and its receptors. FASEB J. *13*, 9–22.

Neufeld, G., Cohen, T., Shraga, N., Lange, T., Kessler, O., and Herzog, Y. (2002). The neuropilins: multifunctional semaphorin and VEGF receptors that modulate axon guidance and angiogenesis. Trends Cardiovasc. Med. *12*, 13–19.

Olsson, A.K., Dimberg, A., Kreuger, J., and Claesson-Welsh, L. (2006). VEGF receptor signalling - in control of vascular function. Nat. Rev. Mol. Cell Biol. *7*, 359–371.

Park, J.E., Keller, G.-A., and Ferrara, N. (1993). The vascular endothelial growth factor (VEGF) isoforms: differential deposition into the subepithelial extracellular matrix and bioactivity of extracellular matrix-bound VEGF. Mol. Biol. Cell *4*, 1317–1326.

Sakurai, Y., Ohgimoto, K., Kataoka, Y., Yoshida, N., and Shibuya, M. (2005). Essential role of Flk-1 (VEGF receptor 2) tyrosine residue 1173 in vasculogenesis in mice. Proc. Natl. Acad. Sci. USA *102*, 1076–1081.

Schueren, F., Lingner, T., George, R., Hofhuis, J., Dickel, C., Gärtner, J., and Thoms, S. (2014). Peroxisomal lactate dehydrogenase is generated by translational readthrough in mammals. eLife *3*, e03640.

Senger, D.R., Galli, S.J., Dvorak, A.M., Perruzzi, C.A., Harvey, V.S., and Dvorak, H.F. (1983). Tumor cells secrete a vascular permeability factor that promotes accumulation of ascites fluid. Science *219*, 983–985.

Shalaby, F., Rossant, J., Yamaguchi, T.P., Gertsenstein, M., Wu, X.F., Breitman, M.L., and Schuh, A.C. (1995). Failure of blood-island formation and vasculogenesis in Flk-1-deficient mice. Nature *376*, 62–66.

Shao, Z., Friedlander, M., Hurst, C.G., Cui, Z., Pei, D.T., Evans, L.P., Juan, A.M., Tahiri, H., Duhamel, F., Chen, J., et al. (2013). Choroid sprouting assay: an ex vivo model of microvascular angiogenesis. PLoS ONE *8*, e69552.

Shevchenko, A., Wilm, M., Vorm, O., and Mann, M. (1996). Mass spectrometric sequencing of proteins silver-stained polyacrylamide gels. Anal. Chem. *68*, 850–858.

Soker, S., Takashima, S., Miao, H.Q., Neufeld, G., and Klagsbrun, M. (1998). Neuropilin-1 is expressed by endothelial and tumor cells as an isoform-specific receptor for vascular endothelial growth factor. Cell *92*, 735–745.

Soker, S., Miao, H.Q., Nomi, M., Takashima, S., and Klagsbrun, M. (2002). VEGF165 mediates formation of complexes containing VEGFR-2 and neuropilin-1 that enhance VEGF165-receptor binding. J. Cell. Biochem. *85*, 357–368.

Tischer, E., Mitchell, R., Hartman, T., Silva, M., Gospodarowicz, D., Fiddes, J.C., and Abraham, J.A. (1991). The human gene for vascular endothelial growth factor. Multiple protein forms are encoded through alternative exon splicing. J. Biol. Chem. *266*, 11947–11954.

Vander Kooi, C.W., Jusino, M.A., Perman, B., Neau, D.B., Bellamy, H.D., and Leahy, D.J. (2007). Structural basis for ligand and heparin binding to neuropilin B domains. Proc. Natl. Acad. Sci. USA *104*, 6152–6157.

Whitaker, G.B., Limberg, B.J., and Rosenbaum, J.S. (2001). Vascular endothelial growth factor receptor-2 and neuropilin-1 form a receptor complex that is responsible for the differential signaling potency of VEGF(165) and VEGF(121). J. Biol. Chem. *276*, 25520–25531.

Woolard, J., Wang, W.Y., Bevan, H.S., Qiu, Y., Morbidelli, L., Pritchard-Jones, R.O., Cui, T.G., Sugiono, M., Waine, E., Perrin, R., et al. (2004). VEGF165b, an inhibitory vascular endothelial growth factor splice variant: mechanism of action, in vivo effect on angiogenesis and endogenous protein expression. Cancer Res. *64*, 7822–7835.

Yu, L., Wu, X., Cheng, Z., Lee, C.V., LeCouter, J., Campa, C., Fuh, G., Lowman, H., and Ferrara, N. (2008). Interaction between bevacizumab and murine VEGF-A: a reassessment. Invest. Ophthalmol. Vis. Sci. *49*, 522–527.

STAR★METHODS

KEY RESOURCES TABLE

REAGENT or RESOURCE	SOURCE	IDENTIFIER
Antibodies		
Anti-VEGF (A-20)	Santa Cruz Biotech, Inc.	Cat#sc-152; RRID: AB_2212984
6x-His epitope tag antibody	Thermo Fisher Scientific	Cat#MA1-21315; RRID: AB_557403
Phosphor-VEGFR2 (Tyr1175)	Cell Signaling Tech. Inc.	Cat#2478S; RRID: AB_331377
Phosphor-VEGFR2 (Tyr951)	Signalway Biotechnol.	Cat#11086; RRID: AB_896080
VEGFR2	Cell Signaling Tech. Inc.	Cat#2479S; RRID: AB_10698606
Phospho-ErK1/2 (Thr202/Tyr204)	Cell Signaling Tech. Inc.	Cat#4376S; RRID: AB_331772
Erk1/2	Cell Signaling Tech. Inc.	Cat#4695S
Anti-Beta-actin (AC-74)	Sigma-Aldrich	Cat#A2228; RRID: AB_476697
Anti-VEGF mAb B20.4.1.	Genentech	N/A
Mouse IgG2a	Bio X Cell	Cat#BE0085; RRID: AB_1107771
Chemicals, Tissue Culture Media, Peptides, and Recombinant Proteins		
Evans blue	Sigma-Aldrich	Cat#E2129
Histamine	Sigma-Aldrich	Cat#H7125
Ketamine	MWI Animal Health	Cat#000680
Xylazine	Lloyd Laboratories	NADA# 139-236
Trypsin	Thermo Fisher Scientific	Cat#90057
GluC	Sigma-Aldrich	Cat#P6181
Ammonium Bicarbonate	Sigma-Aldrich	Cat#40867-50G-F
Acetonitrile	Fisher Scientific	Cat#A995-1
Dithiothreitol (DTT)	Sigma-Aldrich	Cat#10197777001
Iodoacetamide	Sigma-Aldrich	Cat#I1149
Formic Acid	Fisher Scientific	Cat#94318
Trifluoroacetic Acid (TFA)	Fisher Scientific	Cat#28904
NuPAGE® LDS Sample Buffer (4X)	Fisher Scientific	Cat#NP0007
Crystal violet solution	Sigma-Aldrich	Cat#ht90132-1l
Bovine VEGF-Ax, untagged	Ferrara lab	N/A
Bovine His-VEGF-Ax	Ferrara lab	N/A
Human $VEGF_{165}$	R&D Systems	Cat#293-VE
Human VEGF-Ax	R&D Systems	Cat#9018-VE-025/CF
Human $VEGF_{165}b$	R&D Systems	Cat#3045-VE025/CF
Human $VEGF_{121}$	R&D Systems	Cat#4644-VS
Biotinylated $VEGF_{165}$	G&P Biosciences	Cat#FCL0406B
Human basic FGF (bFGF)	PeproTech	Cat#100-18B
Human Neuropilin-1/Fc tag	Sino Biological Inc.	Cat#10011-H02H
HRP Streptavidin	BioLegend	Cat#405210
TMB High Sensitivity Substrate Solution	BioLegend	Cat#421501
Human Fibronectin	Corning	Cat# 356008
Cultrex Reduced Growth Factor Basement Membrane Extract	Trevigen	Cat#3433-005-R1
Dulbecco's Modified Eagle's Medium (high glucose)	Hyclone	Cat#SH30243.01
Dulbecco's Modified Eagle's Medium (low glucose)	Hyclone	Cat#SH30021.01
Bovine calf serum (CS)	Omega Scientific	Cat#BC-04
Fetal bovine serum (FBS)	Omega Scientific	Cat#FB-02
Human Endothelial Serum-Free Medium	GIBCO	Cat#11111-044

(*Continued on next page*)

Continued

REAGENT or RESOURCE	SOURCE	IDENTIFIER
EGM-2 Endothelial Cell Growth Medium	Lonza	Cat#CC3162
EBM-2 Endothelial Cell Basal Medium	Lonza	Cat#CC3156
Critical Commercial Assays		
Bovine VEGF-A ELISA kit	Kingfisher Biotech, Inc.	Cat#VS0286B-002
Pierce protein G IgG plus orientation kit	Fisher Scientific	Cat#PI44990
HisTrap HP column	GE Healthcare	Cat#17-5247-01
SilverQuest silver staining kit	Fisher Scientific	Cat#LC6070
Lipofectamine 3000 transfection reagent	Life Technologies	Cat#L3000075
FreeStyle 293 expression medium	Life Technologies	Cat#12338018
AlamarBlue cell viability assay	Fisher Scientific	Cat#PI88952
Experimental Models: Cell Lines		
Human 293T cells	ATCC	Cat#CRL-11268
Primary human umbilical vein endothelial cells (HUVEC)	Lonza Walkersville Inc.	Cat#C2519AS
Bovine retinal microvascular endothelial cells (BREC)	VEC Technologies	Cat#BRMVEC-3
Bovine choroidal microvascular endothelial cells (BCEC)	VEC Technologies	Cat#BCME-4
Bovine aortic endothelial cells (BAOEC)	Cell Applications	Cat#B304-05
Experimental Models: Organisms/Strains		
Mouse: C57BL/6J (age P20)	Jackson Laboratories	Stock# 000664
Guinea pig: Hairless male guinea pig (450–500 g)	Charles River Laboratories	Crl: HA-Hrhr/IAF
Recombinant DNA		
pcDNA3	Invitrogen	Cat#V790-20
pcDNA3-bVEGF-Ax	Ferrara lab	N/A
pcDNA4(A)/myc-His	Invitrogen	Cat#V863-20
pcDNA4-His-VEGF-Ax	Ferrara lab	N/A
Software and Algorithms		
AxioVision LE Rel.4.4 software	Zeiss	http://www.zeiss.com/microscopy/en_us/downloads/axiovision.html
ImageJ	NIH	https://imagej.nih.gov/ij/
Protein Pilot 5.0 (ABSCIEX)	SCIEX	http://sciex.com/products/software/proteinpilot-software

CONTACT FOR REAGENT AND RESOURCE SHARING

Further information and reagents requests should be addressed to the corresponding author, Napoleone Ferrara (nferrara@ucsd.edu).

EXPERIMENTAL MODELS AND SUBJECT DETAILS

Mice

Twenty-five healthy, naive wild-type C57BL/6J mice were used for mouse choroidal explant assays. Mice (male, age P20) were purchased from Jackson Laboratories and were used on the day of arrival. Animals were housed in clean cages and experimental procedures were carried out under pathogen-free conditions in accordance with established standards of care and approved protocols from the Animal Care and Use Committee of the University of California, San Diego. Prior to tissue harvest, mice were euthanized by CO_2 inhalation followed by cervical dislocation.

Guinea Pigs

Five healthy naive hairless guinea pigs were used for vascular permeability assay. Guinea pigs (Crl: HA-Hrhr/IAF, male, 450–500 g, approximately 2 months old), were purchased from Charles River Laboratories. Animals were individually caged and maintained in pathogen-free conditions in accordance with related guidance and approved protocols from the Animal Care and Use Committee of the University of California, San Diego.

Cells

Human 293T cells were maintained in high glucose Dulbecco's modified Eagle's medium (DMEM) supplemented with 10% fetal bovine serum (FBS). Primary human umbilical vein endothelial cells (HUVEC, passage 4–10, were cultured on 0.1% gelatin-coated plates in EGM-2 endothelial cell growth media. Bovine retinal microvascular endothelial cells (BRECs) and bovine choroidal microvascular endothelial cells (BCECs) were maintained in fibronectin-coated plates (1 $\mu g/cm^2$). The growth medium was low glucose DMEM supplemented with 10% bovine calf serum, 5 ng/ml bFGF and 10ng/ml $hVEGF_{165}$. Bovine aortic endothelial cells were cultured in high glucose DMEM supplemented with 5% fetal bovine serum. Cells were maintained at 37°C in a humidified atmosphere with 5% CO_2.

METHOD DETAILS

Plasmid Construction and Transfection

For construction of VEGF-Ax expression plasmids, a 639-bp nucleic acid fragment of bovine (b) $VEGF\text{-}A_{164}$ and a 22-aminal acid C-terminal extension, in which the canonical stop codon tga was replaced by tcc (serine) (Eswarappa et al., 2014), was synthesized (GenScript USA Inc.) and inserted into pcDNA3 or pcDNA4(A)/myc-His vectors at HindIII/BamHI and Hind III/AgeI sites, generating respectively pcDNA3-VEGF-Ax and pcDNA4-His-VEGF-Ax plasmids. 293T cells were used for transient expression. Transfections were carried out using Lipofectamine 3000 according to the instructions of the manufacturer. The authenticity of all constructs was verified by sequence analysis.

Conditioned Media Preparation and VEGF-A ELISA

Three million 293T cells in 10 cm-dishes were transfected as above described. After 6 hr, cells were washed three times with PBS followed by incubation with 10 ml of serum free medium (FreeStyle 293 expression medium). After 72 hr, media were collected. Aliquots were tested for bioactivity and the bulk was concentrated ten-fold by 10k Amicon centrifugal columns (EMD Millipore) and stored at −80°C until further use. Total VEGF concentrations were measured using a bovine VEGF-A ELISA kit, according to the manufacturer's instructions.

Western Blots

To detect expression of VEGF variants, 25 μL aliquots of conditioned media from 293T cells transiently expressing VEGF-Ax, His-VEGF-Ax or from empty vector-transfected cells, were collected and mixed with NuPAGE® LDS Sample Buffer (4X). The samples were subjected to SDS-PAGE and blotted with anti-VEGF (A-20) or 6x-His Epitope Tag Antibody. To determine phosphorylation of VEGFR2 (tyrosine 951 or 1175) and ERK1/2, HUVECs (passage 6-8) were plated in EBM-2 basal medium with 0.2% FBS. Following overnight culture, cells were serum-starved in EBM-2 medium for 4 hr prior to treatment with 50 ng/ml of VEGF variants or vehicle controls for 10 min. Equal amounts of whole-cell lysates were analyzed by SDS-PAGE and blotted with the indicated antibodies.

Bovine Endothelial Cell Proliferation Assays

Proliferation assays were performed essentially as previously described (Yu et al., 2008). BCECs and BRECs were seeded in 96-well plates (no coating) in low glucose DMEM supplemented with 10% bovine CS, 2 mM glutamine, and antibiotics (growth medium), at a density of 1000 cells per well in 200 μl volume. VEGF-Ax or $VEGF_{165}$ was added at the indicated final concentrations. For VEGF neutralization, 2 μg/ml of anti-VEGF mAb B20.4.1 (Liang et al., 2006) or isotype control IgG2a was first added to triplicate wells. One hour later, VEGF-Ax or wild-type $VEGF_{165}$ was added at the indicated concentrations. After 5 or 6 days, cells were incubated with Alamar Blue for 4h. Fluorescence was measured at 530 nm excitation wavelength and 590 nm emission wavelength. The experiments were repeated at least three times.

VEGF Release from Cultured Bovine Endothelial Cells

To assess total VEGF-A release by cultured bovine endothelial cells, BCECs, BRECs and BAECs (~2 million cells) were plated into 60-mm dishes (1 $\mu g/cm^2$ fibronectin -coated plates for BCECs and BRECs) in low glucose DMEM supplemented with 10% calf serum with 5 ng/ml bFGF and allowed cells grow to 80% confluency. Cells were then washed three times with PBS and incubated with 4 ml of low glucose DMEM supplemented with 2.5% bovine calf serum. Media were collected at 24, 48, 72 and 96h respectively. Media were concentrated 26-fold by 10k Millipore Amicon centrifugal columns prior to ELISA.

HUVEC Migration Assay

HUVECs (passage 6-8) were cultured and serum-starved as described in "Western blots." The cells (10000 cells) in 150 μl of EBM-2 medium were then added to the upper chamber of 8 μm pore size cell culture inserts (Falcon) coated with 0.1% gelatin. The lower compartment was filled with 600 μl EBM-2 medium containing 20 ng/ml $VEGF_{165}$, 50 ng/ml VEGF-Ax or 20 ng/ml $VEGF_{165}$ plus 50 ng/ml VEGF-Ax. The plates were incubated at 37°C to allow migration. After 4h, cells were fixed with 4% PFA for 20 min and then stained with crystal violet for 20 min at RT. Migrated cells on the bottom side of the insert membrane were quantified by counting whole area of the insert at 40X magnification. The experiments were carried out in triplicate and repeated three times.

Scratch Assay

BCECs (passage 6-10) were used in the assay. Cells were cultured in growth medium in 6-well plates until about 80% confluent. They were then washed twice with PBS and incubated in serum-free DMEM for 5 hr before making an incision in the cell monolayers using a 1 ml pipette tip. Cells were washed once with serum-free media, followed by addition of media containing 1% FBS and test molecules. After 48 hr, the assay was stopped by adding 2 ml 4% paraformaldehyde. Twenty minutes later, the fixed cells were stained with 1ml Crystal Violet. Plates were washed gently with water and then air-dried before taking pictures. Images were acquired by ZEISS Discovery V8 SteREO microscopy equipped with PixeLINK Megapixel FireWire camera. Quantification of wound closure was accomplished using AxioVision LE Rel.4.4 software. Six measurements were taken on each field.

Mouse Choroidal Explant Assay

Using pre-cooled pipette tips, 130 μl of reduced growth factor basement membrane extract (BME) was added to each well in a 48-well plate. To avoid evaporation, surrounding wells were filled with PBS. BME was allowed to solidify at 37°C for 20 min. One peripheral sclerochoroidal wedge, dissected from male C57BL/6J (age P20) mice, was added to the center of each well, as previously described (Shao et al., 2013); care was taken to disrupt the tissue minimally. Each experimental condition was tested from explants from a single eye, and was repeated five times. The tissue was incubated at 37°C for 15 min prior to the addition of a top layer of 130 μl BME. After a 30 min incubation period, 500 μl of growth media was added to each well (human endothelial serum free-media containing 2% FBS, 50 units/ml penicillin and 50 μg/ml streptomycin), plus varying concentrations of $VEGF_{165}$ and VEGF-Ax. Explants were incubated in standard cell culture conditions with 5% CO_2. Fresh media was exchanged at day 2 and day 4. Images were taken on day 4 and day 6 using an inverted microscope with a 10X objective and acquired using Axiovision software.

Vascular Permeability Assay

Vascular permeability was assessed using a modified Miles assay (Gille et al., 2001). Hairless male guinea pigs (Crl: HA-Hr^{hr}/IAF, 450–500 g, Charles River Laboratories) were anesthetized by intraperitoneal (i.p.) administration of xylazine (5 mg/kg) and ketamine (75 mg/kg). The animals then received an intravenous injection (penile vein) of 1 ml of 1% Evans blue dye. After ~15 min, intradermal injections (0.05 ml/per site) of different doses (0, 25, 50, 100, 250 ng per injection site) of VEGF-Ax, $VEGF_{165}$ and a combination of 50 ng $VEGF_{165}$ with different doses of VEGF-Ax (0, 25, 50, 100, 250 ng) were administrated into the area of trunk posterior to the shoulder. VEGF-Ax and $VEGF_{165}$ were diluted in PBS for intradermal administration. 1.5 μg per site of histamine was used as positive control. 30 min after the intradermal injections, animals were euthanized by i.p. injection of pentobarbital (200 mg/kg). Skin tissues were dissected from the connective tissues and photographed. Quantification of the dye extravasation area was carried out on the pictures using ImageJ image analysis software. For each dose, measurements were made in total five animals.

Purification of VEGF-Ax

Untagged VEGF-Ax was purified from conditioned media of 293T cells transiently expressing pcDNA3-VEGF-Ax plasmid using an anti-VEGF antibody column. The column was prepared using the Pierce Protein G IgG Plus Orientation Kit according to the manufacturer's instructions. Briefly, 16 mg of anti-VEGF-A mAb B20.4.1 (Liang et al., 2006) (Genentech Inc, South San Francisco, CA) was used to bind 2 ml Protein G agarose and cross-linked by treatment with DSS. The resin was then packed into a GE Healthcare Tricorn 10/50 Column. Up to 300 μg VEGF-Ax by ELISA were loaded and purified using a GE AKTA Explorer System. After loading, the column was stepwise washed with 20 mM Tris pH 7.2, containing 0.15 and 0.6 M NaCl and eluted with 0.1 M glycine•HCl, pH 2.8, which was immediately neutralized with 1M Tris•HCl, pH 9.5. His-VEGF-Ax was purified from conditioned media of 293T cells transiently expressing pcDNA4-His-VEGF-Ax plasmid by HisTrap ^{HP} columns (1ml or 5ml) (GE Healthcare). Conditioned media were exchanged into binding buffer (20 mM NaH_2PO_4, 0.5 M NaCl, 20 mM imidazole). After stepwise washing with 50 and 100 mM imidazole, VEGF-Ax was eluted with 20 mM NaH_2PO_4, 500 mM NaCl, 500 mM imidazole. Buffers was exchanged into PBS by PD-10 columns (GE Healthcare). VEGF-Ax concentrations in the fractions were measured by ELISA and the purity of the proteins were assessed by silver-stained SDS-PAGE.

Structural Analysis

For in-gel digest and mass spectrometry (MS) analysis (Shevchenko et al., 1996), 3 μg of purified untagged VEGF-Ax were subjected to SDS-PAGE and silver-stained using a MS-compatible kit (Silverquest, Fisher Scientific). Two bands in reducing conditions, the major of about 25 kDa and the minor, a doublet of ~18-20kDa, were cut from the gel and destained. The samples were separately subjected to digestion with trypsin and GluC and analyzed as described below.

In Gel Digest

The gel slices were cut to 1mm by 1mm cubes and destained 3 times by first washing with 100 μl of 100 mM ammonium bicarbonate for 15 min, followed by addition of the same volume of acetonitrile (ACN) for 15 min. The supernatant was removed and samples were dried in a speedvac. Samples were then reduced by mixing with 200 μl of 100 mM ammonium bicarbonate-10 mM DTT and incubated at 56°C for 30 min. The liquid was removed and 200 μl of 100mM ammonium bicarbonate-55 mM iodoacetamide was added to gel pieces and incubated at room temperature in the dark for 20 min. After the removal of the supernatant and one wash with 100mM ammonium bicarbonate for 15 min, same volume of ACN was added to dehydrate the gel pieces. The solution was then removed and samples were dried in a speedvac. For digestion, enough solution of ice-cold trypsin (0.01 μg/μl) in 50 mM ammonium bicarbonate or

GluC for C-terminal sequencing (0.01 μg/μl) was added to cover the gel pieces and set on ice for 30 min. After complete rehydration, the excess protease solution was removed, replaced with fresh 50 mM ammonium bicarbonate, and left overnight at 37°C. The peptides were extracted twice by the addition of 50 μl of 0.2% formic acid and 5% ACN and vortex mixing at room temperature for 30 min. The supernatant was removed and saved. A total of 50 μl of 50% ACN-0.2% formic acid was added to the sample, which was vortexed again at room temperature for 30 min. The supernatant was removed and combined with the supernatant from the first extraction. The combined extractions are analyzed directly by liquid chromatography (LC) in combination with tandem mass spectroscopy (MS/MS) using electrospray ionization.

LC-MS-MS

Trypsin-digested peptides were analyzed by ultra high pressure liquid chromatography (UPLC) coupled with tandem mass spectroscopy (LC-MS/MS) using nano-spray ionization. The nanospray ionization experiments were performed using a TripleTof 5600 hybrid mass spectrometer (ABSCIEX) interfaced with nano-scale reversed-phase UPLC (Waters corporation nano ACQUITY) using a 20 cm-75 micron ID glass capillary packed with 2.5-μm C18 CSH beads (Waters corporation). Peptides were eluted from the C18 column into the mass spectrometer using a linear gradient (5%–80%) of ACN at a flow rate of 250 μl/min for 1h. The buffers used to create the ACN gradient were: Buffer A (98% H_2O, 2% ACN, 0.1% formic acid, and 0.005% TFA) and Buffer B (100% ACN, 0.1% formic acid, and 0.005% TFA). MS/MS data were acquired in a data-dependent manner in which the MS1 data were acquired for 250 ms at m/z of 400 to 1250Da and the MS/MS data were acquired from m/z of 50 to 2,000 Da. The Independent data acquisition (IDA) parameters were as follows; MS1-TOF acquisition time of 250 ms, followed by 50 MS2 events of 48 ms acquisition time for each event. The threshold to trigger MS2 event was set to 150 counts when the ion had the charge state +2, +3 and +4. The ion exclusion time was set to 4 s. Finally, the collected data were analyzed using Protein Pilot 5.0 for peptide identifications.

Solid-Phase NRP1 Binding Assay

Costar 96-well EIA/RIA stripwells (Immunochemistry Technologies) were coated overnight at 4°C with 5 μg/ml human NRP1 (Fc-tagged). Nonspecific binding sites were blocked by incubating the strips with 2% BSA in PBS for 1 hr at room temperature (RT) after single wash, followed by addition of 50 ng/ml biotinylated $VEGF_{165}$ alone or in combination with various concentrations (50-1000 ng/ml) of non-biotinylated $VEGF_{165}$, $VEGF_{121}$ or VEGF-Ax at 37°C for 2 hr. After three washes, bound biotinylated $VEGF_{165}$ was detected by incubation with HRP Streptavidin (1:1000) for 1 hr at RT. Strips were extensively washed before incubation with TMB high sensitivity substrate solution (Biolegend) for 30min, and absorbance at 450nm was measured after adding equal amounts of stop solution (Biolegend). All experiments were carried out in duplicate and repeated three times.

QUANTIFICATION AND STATISTICAL ANALYSIS

Statistical parameters, including the value of n, are indicated in the figure legends. The 2-tailed Student's *t* test was used for statistical analysis. Data are considered significant when $p < 0.05$. Significant p values are represented in the figures as follows: ***$p < 0.001$, **$p < 0.01$, *$p < 0.05$.

Cell

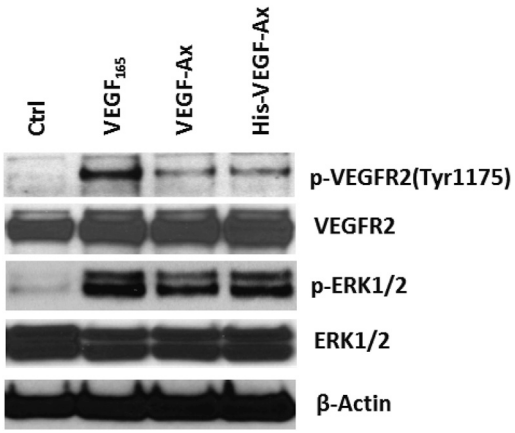

Figure S1. Activation of VEGFR2 Signaling, Related to Figure 3

Activation of VEGFR2 signaling. Western blot showing phosphorylation of VEGFR2 and ERK1/2 induced by untagged VEGF-Ax, His-VEGF-Ax or $VEGF_{165}$ in HUVECs. Serum-starved HUVECs were stimulated with 50 ng/mL of VEGF variants for 10 min. PBS was used as control. Equal amounts of whole-cell lysates were subjected to SDS-PAGE and then blotted by the indicated antibodies.